

Attraction and Repulsion of Nucleons: Sources of Stellar Energy

O. Manuel¹, C. Bolon¹, A. Katragada¹, and M. Insall¹

The potential energy of a nuclide is enhanced by about 10 MeV per nucleon from the repulsion between like nucleons and diminished by about 20 MeV per nucleon from the attraction between unlike nucleons. Nuclear stability results mostly from the interplay of these opposing forces, plus Coulomb repulsion of positive charges. While fusion may be the primary mechanism by which first generation stars produce energy, repulsion between like nucleons may cause neutron emission from the collapsed core (neutron star) produced in a terminal supernova explosion and initiate luminosity in second generation stars that accrete on such objects. As noted earlier [1], the scarcity of solar neutrinos, the enrichment of light isotopes in the solar wind, and, the presence of abundant short-lived nuclides and inter-linked chemical and isotopic heterogeneities in the early solar system might also be explained if the Sun formed in this manner.

KEY WORDS: Nucleon interactions; fusion; neutron emission; solar energy

I. INTRODUCTION

In 1917 Harkins [2] used meteorites to determine the abundance of elements. He found that seven elements - iron (Fe), oxygen (O), nickel (Ni), silicon (Si), magnesium (Mg), sulfur (S), and calcium (Ca) - comprise 99% of the material in ordinary meteorites and *"all of these elements have even atomic numbers"* (p. 862). He suggested a link between elemental abundance and nuclear stability, noting that *"... in the evolution of elements much more material has gone into the even-numbered elements than into those which are odd..."* (p. 869).

In the 1920s, Payne [3] and Russell [4] reported that the Sun's atmosphere

consisted mostly of hydrogen (H) and helium (He), but Hoyle [5] notes that he and others *"in the astronomical circles to which I was privy"* (p. 153) continued until after the Second World War to believe that the Sun was made mostly of iron. Then Hoyle notes that *"much to my surprise"* (p. 154), the high-hydrogen, low-iron model was suddenly adopted without opposition.

Perhaps research on H-fusion for thermonuclear weapons lead scientists to revise their opinions about the interior of the Sun. Teller [6] reports that Gamow, Critchfield and Bethe had concluded that fusion reactions *"... keep stars going"* (p. 67) before the discovery of fission in December of 1938 and *"We were all convinced ... that we could accomplish a thermonuclear explosion"* and this was *"one*

¹University of Missouri, Rolla, MO 65401 USA (om@umr.edu)

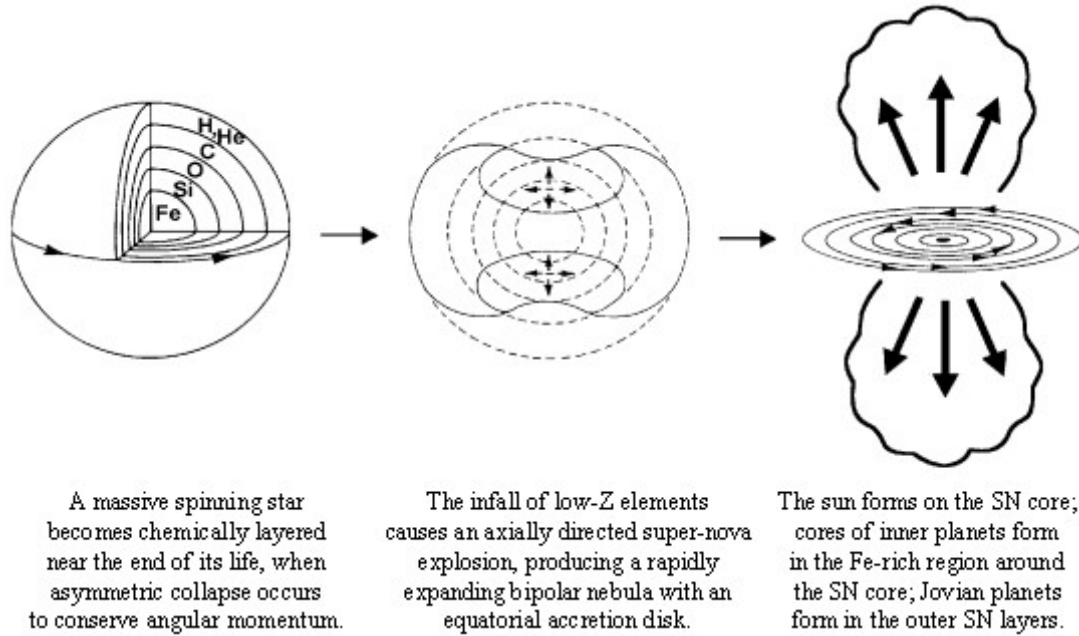


Fig. 1. One suggested scenario [13] to explain inter-linked chemical and isotopic heterogeneities and the decay products of short-lived nuclides in meteorites. SN = supernova.

of the laboratory's objectives" (p. 70) when the Los Alamos Laboratory was established in 1943. The new weapon from Los Alamos in 1945 was based on a fission explosion that was later to provide the trigger for the hydrogen bomb.

In 1969, the Apollo 11 crew returned to Earth with lunar samples replete with volatile elements [7] implanted by the solar wind (SW). By then the homogeneous, H-rich model of the Sun had been widely accepted for several years. Consequently fourteen years elapsed before, in 1983, possible evidence of an iron-rich Sun was recognized in the SW-implanted elements.

In the intervening years, evidence of fresh stellar debris had been found in the isotopes of many different elements trapped in meteorites [8], beginning with the discovery of radiogenic ^{129}Xe , the decay product of extinct ^{129}I [9], and a primordial isotopic anomaly pattern [10] across the other eight, stable Xe isotopes.

By the mid-1970's, Clayton [11] had noted that this profusion of nuclear reactions

might have been recorded by interstellar grains embedded in meteorites. Others [12] proposed to explain these observations by the explosion of a nearby supernova (SN) that injected alien nucleogenetic material into the early solar system. Another group [13] suggested the possibility that our solar system might have formed directly from the debris of a single supernova. In this hypothetical scenario, illustrated in Fig. 1, cores of the inner planets formed in a central iron-rich region and the Sun formed on the collapsed SN core.

Hence meteorite analyses revived the concept of an iron-rich Sun in the 1970's, almost a decade prior to publication of a report noting that each light weight noble gas isotope (m_L) in SW-exposed lunar samples is enriched relative to any heavier isotope (m_H) by a factor (f) with a common functional dependency, where the value of f is given by an empirical power law [14]:

$$f = (m_H/m_L)^{4.56} \quad (1)$$

When this empirical mass-

fractionation relationship, defined by the enrichments of light isotopes of SW-implanted helium (He), neon (Ne), argon (Ar), krypton (Kr), and xenon (Xe), was applied to photospheric abundances, the most abundant elements in the unfractionated, bulk Sun were predicted to be, in decreasing order, Fe, Ni, O, Si, S, Mg and Ca [14, 15]. These elements are made deep in the interior of supernovae. They are the

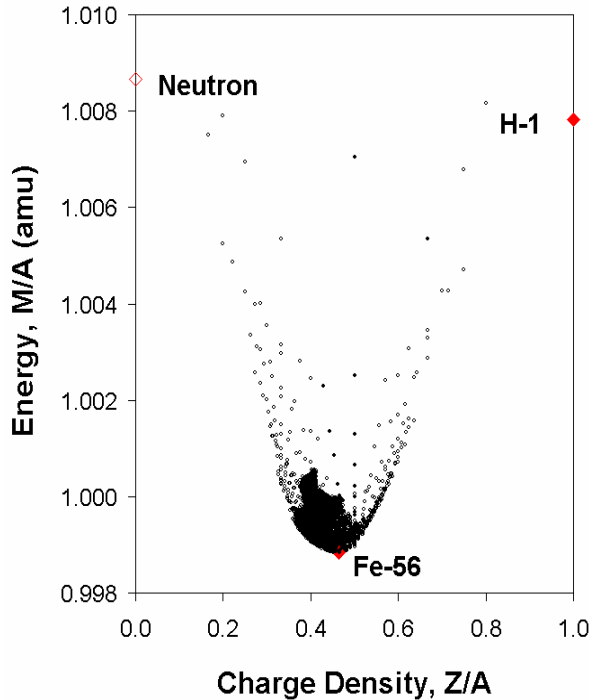


Fig. 2. A plot of mass per nucleon, M/A , versus charge per nucleon, Z/A , for all nuclides in the 2000 edition of Nuclear Wallet Cards. Radioactive nuclides are represented by open symbols; stable and long-lived nuclides are represented by filled symbols.

same elements Harkins [2] found to comprise 99% of the material in ordinary meteorites, but they are only trace elements in the Sun's photosphere. Purely random selection of these same seven elements, by the application of Eq. (1) to photospheric abundances, is highly improbable [1].

However the Fe/H ratio predicted for the bulk Sun, by the application of Eq. (1) to photospheric abundances, is even higher than that assumed prior to the end of the Second World War [5]. In the present

paper, interactions between nucleons are examined to see if these might explain the luminosity of an Fe-rich, H-poor stellar object.

II. INTERACTIONS BETWEEN NUCLEONS

Fig. 2 is a plot of charge density (Z/A) on the horizontal axis, and energy per nucleon (M/A) on the vertical axis for all nuclides in the sixth edition of Nuclear Wallet Cards [16]. Open symbols represent radioactive nuclides; filled symbols represent stable and long-lived nuclides.

Most nuclides lie within a triangle bounded by three nuclides with extreme values of M/A and Z/A . The neutron (on the left) has the largest value of M/A and the lowest value of Z/A of any nuclide. The Fe-56 nuclide (near the center) has the lowest value of M/A . The H-1 atom (on the right) has the highest value of Z/A . It also has the highest value of M/A among stable and long-lived nuclides.

The data in Fig. 2 can be sorted by mass number, A , or atomic number, Z , or neutron number, N , to show the relationship between energy and charge density for isobars, isotopes, or isotones [17].

[17].

Fig. 3 is the family of isobaric mass parabolas defined by the data after sorting those in Fig. 2 into a third dimension represented by the mass number, A . The more stable nuclides lie along the valley of this trough, the "Cradle of the Nuclides" [1, 17]. Nuclides that are radioactive or are readily destroyed by fusion or fission occupy higher positions in the cradle.

A slice through this cradle at any given value of A yields the familiar isobaric mass parabola. This is illustrated in Fig. 4 for $A = 27$. This is a typical, odd- A mass parabola, and it is useful for illustrating the interactions between nucleons.

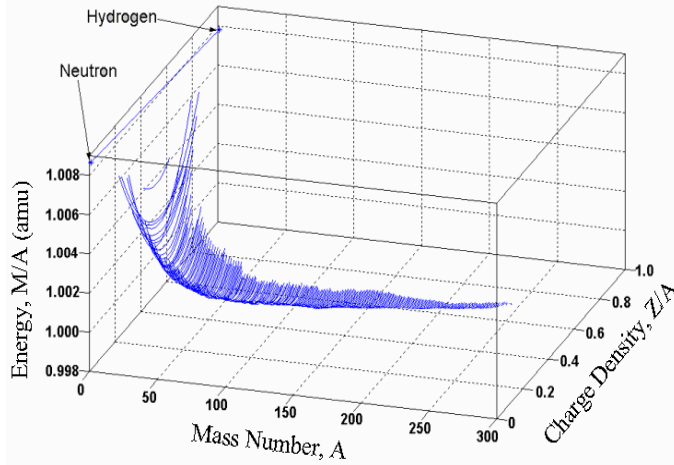


Fig. 3. The family of isobaric mass parabolas defined by the nuclear mass data after sorting into a third dimension represented by the mass number, A

For comparison, the values of M/A are also shown in Fig. 4 for the two unbound nucleons, ${}^1_0\text{n}$ and ${}^1_1\text{H}$ at $Z/A = 0$ and $Z/A = 1$, respectively.

The Coulomb energy, E_C , from the repulsion between positive nuclear charges increases from left to right in Fig. 4 as the number of protons increases. Owing to a large contribution from E_C , the value predicted for M/A on the right side of the figure is off-scale, for example, at $Z/A = 1.0$ where the nucleus consists only of 27 protons in ${}^{27}_{11}\text{Co}$. This Coulombic repulsion between positive charges may be the best understood interaction between nucleons.

To elucidate the other interactions between nucleons, the contribution of E_C was first subtracted from each known nuclide mass at $A = 27$: ${}^{27}_{11}\text{F}$, ${}^{27}_{10}\text{Ne}$, ${}^{27}_{9}\text{Na}$, ${}^{27}_{8}\text{Mg}$, ${}^{27}_{7}\text{Al}$, ${}^{27}_{6}\text{Si}$, ${}^{27}_{5}\text{P}$, ${}^{27}_{4}\text{S}$. For this correction, we used the recently determined value [18] of E_C , namely, $E_C = 0.702 \text{ MeV} (Z^2/A^{1/3})$.

Fig. 5 shows the "best fit" mass parabola after subtracting Coulomb energy, E_C , from the rest mass of each of the eight known isobars at $A = 27$. Note that this correction for E_C also reduces the rest mass

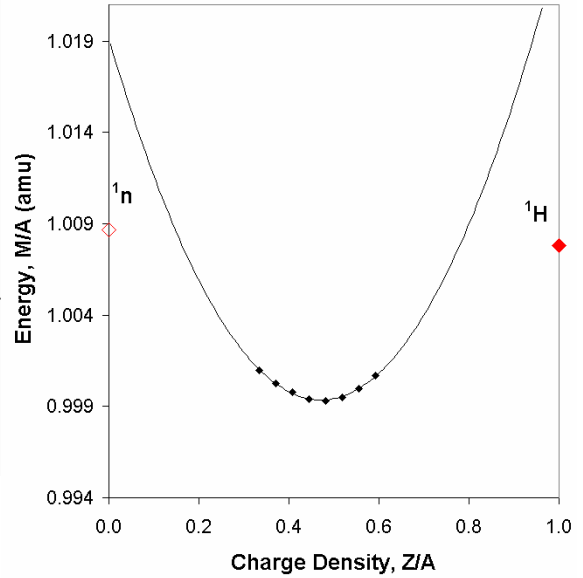


Fig. 4. The parabola defined by the mass per nucleon versus charge density for the isobars at $A = 27$. Values of M/A are shown for unbound nucleons on the left at $Z/A = 0$ for ${}^1_0\text{n} = 1.008665 \text{ amu}$ and on the right at $Z/A = 1$ for ${}^1_1\text{H} = 1.007825 \text{ amu}$

of the ${}^1_1\text{H}$ nuclide, shown on the right side of Fig. 5, from 1.007825 amu to 1.007071 amu .

After correcting for Coulomb energy, the parabola is more symmetrical. Its shape suggests that the n-n and p-p interactions are about equal and repulsive, increasing the average energy per nucleon above that of free nucleons, while the n-p interactions are attractive, decreasing the average energy per nucleon below that of the unbound nucleons.

The n-n and p-p interactions seem to be nearly identical. This may explain why, before subtraction of E_C , the differences between values of M/A at the intercepts (where $Z/A = 0$ and $Z/A = 1$) varied in a regular manner with A in just the manner expected from differences in E_C [18]. In the case illustrated in Fig. 5, the intercept values of M/A after subtraction of E_C are

$$(M/A)_{Z/A=0} = M({}^1_0\text{n}) + 9.76 \text{ Mev, and}$$

$$(M/A)_{Z/A=1} = M({}^1_1\text{H} - E_C) + 9.71 \text{ Mev.}$$

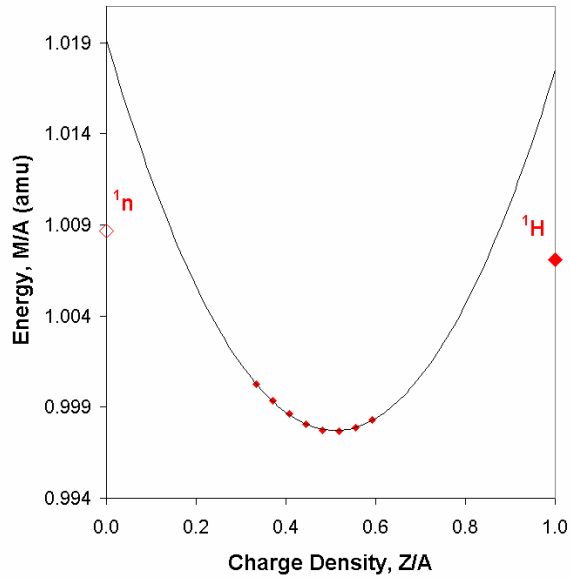


Fig. 5. The mass per nucleon parabola for the isobars at $A = 27$ after subtracting Coulomb energy, E_C . Values of M/A are again shown for unbound nucleons, on the left at $Z/A = 0$ for ${}^1_0\text{n} = 1.008665$ amu and on the right at $Z/A = 1$ for ${}^1_1\text{H} - E_C = 1.007071$ amu.

Symmetry of the n-n and p-p interactions is also suggested by comparing the ratio of the masses of the unbound nucleons to the ratio of the extrapolated masses on the parabola at the intercepts in Fig. 5,

$$\frac{(M/A)_{Z/A=0}}{(M/A)_{Z/A=1}} = 1.0000 \frac{M({}^1_0\text{n})}{M({}^1_1\text{H} - E_C)}$$

Thus, the potential energy of neutrons and protons each seem to increase by about 10 MeV per nucleon in the presence of like nucleons, in addition to any changes caused by Coulombic interactions.

Countering this disruptive force between like nucleons is an attractive interaction between unlike nucleons. In a nuclide consisting of Z protons and N neutrons, if each nucleon interacts with every other nucleon in the nucleus then the number of n-n interactions would be $(N)(N-1)/2$, the number of p-p interactions would

be $(Z)(Z-1)/2$, and the number of n-p interactions would be $(N)(Z)$.

Table I shows the number of n-n, p-p, and n-p interactions for each isobar at $A = 27$. Column 6 in Table I gives a weighted net number of interactions, assuming that the n-n and p-p interactions are equal and that the n-p interactions have an opposing contribution that is empirically estimated to be 2.5 times greater than either the n-n or p-p interactions.

Table I. Interactions between nucleons at $A = 27$

| No. Z | No. N | No. n-n | No. p-p | No. n-p | $\Sigma (n-n) + (p-p) - 2.5(n-p)$ |
|-------|-------|---------|---------|---------|-----------------------------------|
| 0 | 27 | 351 | 0 | 0 | +351 |
| 1 | 26 | 325 | 0 | 26 | +260 |
| 2 | 25 | 300 | 1 | 50 | +176 |
| 3 | 24 | 276 | 3 | 72 | +96 |
| 4 | 23 | 253 | 6 | 92 | +29 |
| 5 | 22 | 231 | 10 | 110 | -34 |
| 6 | 21 | 210 | 15 | 126 | -90 |
| 7 | 20 | 190 | 21 | 140 | -139 |
| 8 | 19 | 171 | 28 | 152 | -181 |
| 9 | 18 | 153 | 36 | 162 | -216 |
| 10 | 17 | 136 | 45 | 170 | -244 |
| 11 | 16 | 120 | 55 | 176 | -265 |
| 12 | 15 | 105 | 66 | 180 | -279 |
| 13 | 14 | 91 | 78 | 182 | -286 |
| 14 | 13 | 78 | 91 | 182 | -286 |
| 15 | 12 | 66 | 105 | 180 | -279 |
| 16 | 11 | 55 | 120 | 176 | -265 |
| 17 | 10 | 45 | 136 | 170 | -244 |
| 18 | 9 | 36 | 153 | 162 | -216 |
| 19 | 8 | 28 | 171 | 152 | -181 |
| 20 | 7 | 21 | 190 | 140 | -139 |
| 21 | 6 | 15 | 210 | 126 | -90 |
| 22 | 5 | 10 | 231 | 110 | -34 |
| 23 | 4 | 6 | 253 | 92 | +29 |
| 24 | 3 | 3 | 276 | 72 | +96 |
| 25 | 2 | 1 | 300 | 50 | +176 |
| 26 | 1 | 0 | 325 | 26 | +260 |
| 27 | 0 | 0 | 351 | 0 | +351 |

Fig. 6 is a plot of the weighted net interactions versus charge density for all 28 isobars at $A = 27$. The excellent match between Fig. 5 and Fig. 6 seems to confirm that the number of interactions between nucleons governs nuclear stability and that the n-n and p-p interactions are symmetrical, repulsive and less than half as strong as the

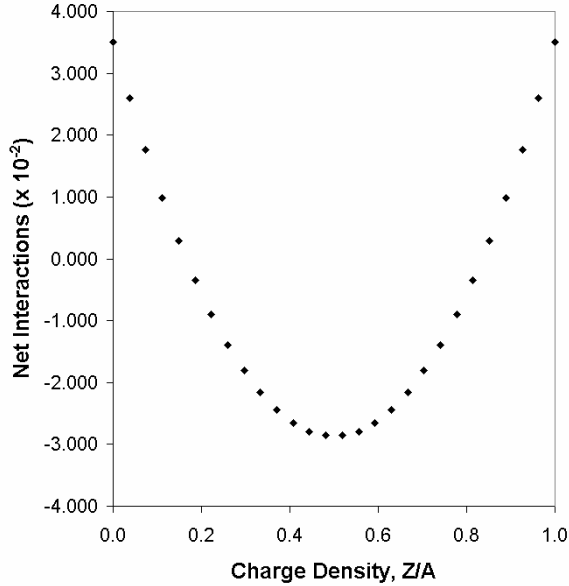


Fig. 6. A hypothetical mass parabola at $A = 27$ obtained by assuming that the interactions between nucleons tabulated in Table I generate the mass parabola. To match the empirical trends shown in Fig. 5, the n-n and p-p interactions are assumed to be repulsive and equal while the n-p interaction is attractive and 2.5 times stronger. These net interactions are shown in Column six of Table I.

attractive n-p interactions at $A = 27$.

In comparing the values of M/A at different values of A , two other terms must be considered. The probability that a given nucleon will interact with any of the other $A-1$ nucleons is $1/(A-1)$, and the net effect *per nucleon* will also have the factor $1/A$. The net effect, $1/A(A-1)$, is constant at any given value of A , as in Figs. 4, 5 and 6, but the number of nucleon interactions divided by $A(A-1)$ should be used in comparing nuclides of different mass number.

Interactions between nucleons have a decreased effect on values of M/A (potential energy per nucleon) for lower values of A . The weak binding of nucleons in ${}^2\text{H}$ illustrates this for the n-p interaction. The six known isotopes of hydrogen [15] show this for the n-n interactions.

Fig. 7 shows the values of M/A versus Z/A for the six isotopes of Hydrogen

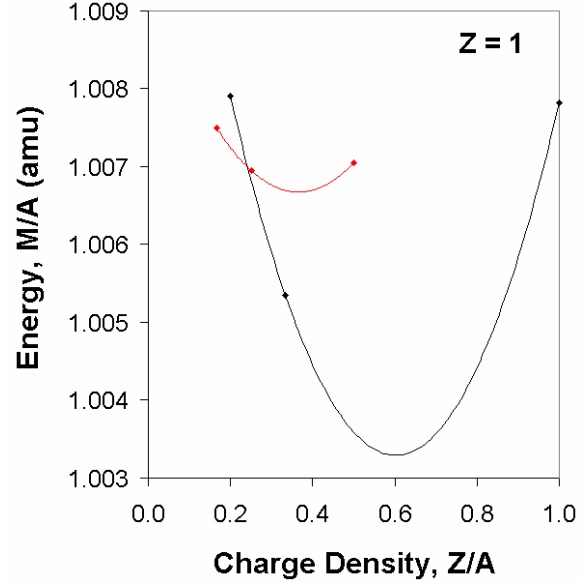


Fig. 7. The six isotopes of hydrogen on a plot of mass per nucleon versus charge density. The three isotopes with odd numbers of neutrons, ${}^6\text{H}$, ${}^4\text{H}$, and ${}^2\text{H}$, define the shallow parabola on the left; the three isotopes with even numbers of neutrons, ${}^5\text{H}$, ${}^3\text{H}$, and ${}^1\text{H}$, define the deeper parabola on the right. The intercepts at $Z/A = 0$ yield values $M/A = M({}^1\text{n}) + 0.7$ MeV for the parabola on the left and $M/A = M({}^1\text{n}) + 4.6$ MeV for the parabola on the right.

isotopes with odd numbers of neutrons (${}^6\text{H}$, ${}^4\text{H}$ and ${}^2\text{H}$) define the shallow parabola on the left. Those with even numbers of neutrons (${}^5\text{H}$, ${}^3\text{H}$ and ${}^1\text{H}$) define the deeper parabola on the right. At $Z/A = 0$, the shallow parabola yields an intercept of $M/A = M({}^1\text{n}) + 0.7$ MeV. The other parabola yields an intercept of $M/A = M({}^1\text{n}) + 4.6$ MeV. Both of these are substantially less than the intercepts for higher values of Z . Interactions between odd numbered neutrons in H seem especially weak.

III. FUSION AND DISSOCIATION AS SOURCES OF STELLAR ENERGY

The interactions concluded here between nucleons offer new insight into the source of stellar energy. Fusion has been widely believed to be the energy source for

the Sun and other stars. Burbidge *et al.* [19] showed that elemental and isotopic abundances in the solar system could be understood in terms of reasonable nuclear reactions that might occur as a first generation star, consisting initially of hydrogen, underwent normal stages of stellar evolution up to and including its terminal explosion as a supernova (SN).

If the Sun, a second generation star, formed on the collapsed SN core, as shown in Fig. 1, then repulsion between neutrons could be the driving force for neutron emission from the collapsed core of the supernova that produced our elements. This may be the first, and the rate-determining, step in the production of solar luminosity and the Sun's outward flow of solar-wind (SW) protons [15]:

- a) Escape of neutrons from the collapsed SN core;
- b) Decay of free neutrons or capture by other nuclides;
- c) Fusion of most H^+ during its upward migration, carrying lighter elements and the lighter isotopes of each element to the solar surface; and finally the
- d) Annual escape of $3 \times 10^{43} H^+$ in the solar wind.

Fig. 8 illustrates how the attractive and repulsive interactions between nucleons might generate energy in first and second generation stars.

CONCLUSIONS

The attractive force between unlike nucleons may allow first generation stars to generate energy by fusion. The repulsive force between like nucleons may allow the collapsed cores of first generation stars to generate energy by neutron emission. The

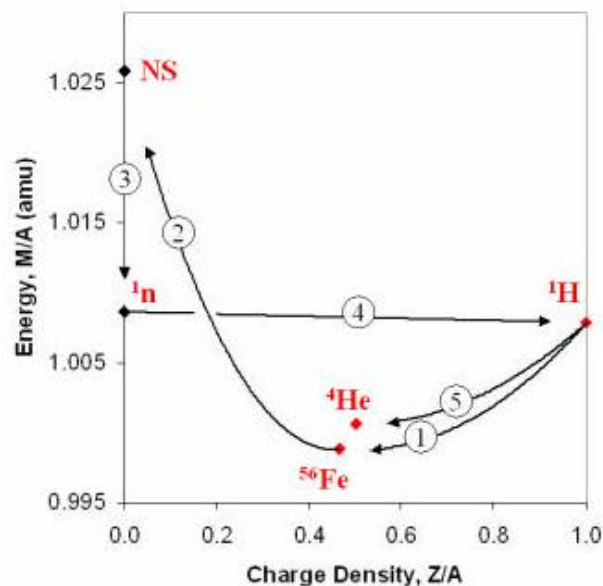


Fig. 8. Nuclear evolution in the Sun and in first generation stars, illustrated on a plot of M/A vs. Z/A . (1) First generation stars fuse 1H into heavier nuclides. (2) At the end of their life, material in the core may be compressed into a neutron star (NS). Our Sun, a second generation star, may have formed on this product [13]. (3) The NS acts as a giant nucleus [15], decaying with the emission of neutrons ($Q = 10^{-22}$ MeV/neutron; $t_{1/2} \sim 10^{10}$ years). (4) After $^1H \rightarrow ^1n$ decay, the 1H -atoms migrate upward, carrying lighter elements and lighter isotopes of each element to the solar surface [14]. (5) En route, most of the 1H -atoms are consumed by fusion. The small fraction that reaches the surface generate a solar wind flux of $3 \times 10^{43} H^+$ per year.

Sun and other second generation stars that formed by the accretion of material on collapsed SN cores may generate energy by neutron emission, followed by fusion.

ACKNOWLEDGMENTS

This work was supported by The Foundation for Chemical Research, Inc., which also kindly granted permission to reproduce Figs. 2-8 here. Fig. 1 is reproduced from the abstract of a paper presented at the 32nd Lunar and Planetary

Science Conference [15]. We are also grateful to Mr. Joseph Council for all of his assistance.

REFERENCES

1. O. Manuel (2000). in *Origin of Elements in the Solar System: Implications of Post-1957 Observation* (Kluwer Academic/Plenum Publishers, New York, NY) Proceedings of the ACS Symposium organized by Glenn T. Seaborg and Oliver K. Manuel, pp. 589-643. See web page at <http://www.wkap.nl/book.htm/0-306-46562-0>
2. W. D. Harkins (1917). *J. Am. Chem. Soc.* **39**, 856-879.
3. H. H. Payne (1926). "Stellar atmospheres", *Harvard Observatory Monograph*, no. 1 (Harvard University, Cambridge, MA) 215 pp.
4. H. N. Russell (1929). *Ap. J.* **70**, 11-82.
5. Fred Hoyle (1994). *Home Is Where the Wind Blows* (University Science Books, Mill Valley, CA) pp. 152-154.
6. Edward Teller (1987). *Better A Shield Than A Sword* (Macmillian, New York, NY) 257 pp.
7. The Lunar Sample Preliminary Examination Team (1969). *Science* **165**, 1211-1227.
8. F. Begemann (1980). *Rep. Prog. Phys.* **43**, 1309-1356.
9. J. H. Reynolds (1960). *Phys. Rev. Lett.* **4**, 8-10.
10. J. H. Reynolds (1960). *Phys. Rev. Lett.* **4**, 351-354.
11. D. D. Clayton (1975). *Ap. J.* **199**, 765-769.
12. G. W. Cameron and J. W. Truran (1977). *Icarus* **30**, 447-461.
13. O. K. Manuel and D. D. Sabu (1975). *Trans. Missouri Acad. Sci.* **9**, 104-122; (1977). *Science* **195**, 208-209.
14. O. K. Manuel and G. Hwaung (1983). *Meteoritics* **18**, 209-222.
15. O. Manuel, C. Bolon, M. Zhong, and P. Jangam (2001). Abstract 1041, *Lunar Planetary Science Conference XXXII*, LPI Contribution No. 1080, ISSN No. 0161-5297.
16. J. K. Tuli (2000). *Nuclear Wallet Cards*, Sixth Edition, Upton, NY: National Nuclear Data Center, Brookhaven National Lab, 2000, 74 pp.
17. O. Manuel, C. Bolon, M. Zhong, and P. Jangam (2000). "The Sun's origin, composition and source of energy," Progress report to FCR, Inc., http://www.umr.edu/~om/report_to_fcr/report_to_fcr1.htm, December 25, 2000.
18. O. Manuel, C. Bolon, and M. Zhong (2001). *J. Radioanal. Nucl. Chem.*, in press.
19. E. M. Burbidge, G. R. Burbidge, W. A. Fowler and F. Hoyle (1957). *Rev. Mod. Phys.* **29**, 547-650.